Table XII. Reduction Potentials (V vs SCE) of Various Five-Coordinated Fe(III) Octaethylporphyrin Complexes in CH_2Cl_2 Containing $(TBA)ClO_4$ or $(TBA)PF_6$ as Supporting Electrolyte

axial ligand	type of bond	spin state[a]	$E_{1/2}$	ref
ClO_4^-	ionic	is, hs	0.10	59
$N_4C(C_2H_5)$	σ	hs	-0.32	this work
Br^-	ionic	hs	-0.34	59
$N_4C(CH_3)$	σ	hs	-0.37	this work
Cl^-	ionic	hs	-0.42	59
N_3^-	ionic	hs	-0.52	this work
F^-	ionic	hs	-0.63	59
C_6F_4H	σ	hs	-0.64[b]	46
C_6F_5	σ	hs	-0.66[b]	46
C_6H_5	σ	ls	-0.91	68

[a] Key: is = intermediate spin; hs = high spin; ls = low spin. [b] Irreversible reaction. Value listed is E_p at a scan rate of 0.1 V/s.

iron atom, while delocalization of the unpaired electron spin from the d_{xz} and d_{yz} orbitals toward the $4e(\pi^*)$ porphyrin orbitals induces a π spin density on the meso site.[75] The contact shifts of the axial tetrazolato substituents are indicative of a low σ spin density. The magnitude of the contact contribution also appears to be strongly dependent upon the nature of the axial ligand (see Table XI).

In the preceding paper,[26] potentials for electroreduction were used to evaluate the relative metal-ligand bond strength of various (TPP)InX, (TPP)In(R), and (TPP)In[$N_4C(R)$] complexes. The most easily reduced In(III) porphyrins are those with ionic or tetrazolato axial ligands, while the most difficult to reduce are those with σ-bonded alkyl or aryl axial ligands. The same order is observed for iron(III) porphyrins, but for these complexes the effect of metal spin state must also be considered in evaluating the trends of $E_{1/2}$ with changes in metal-ligand bond strength.

A summary of potentials for reduction of 10 representative pentacoordinated Fe(III) OEP complexes is given in Table XII. Each compound undergoes an Fe(III) → Fe(II) reduction at a potential that is strongly dependent upon the axial ligand field strength as well as upon the spin state of the central metal. The most easily reduced Fe(III) porphyrin is $(OEP)FeClO_4$ ($E_{1/2}$ = +0.10 V), while the most difficult is $(OEP)Fe(C_6H_5)$ ($E_{1/2}$ = -0.91 V). The perchlorate derivative contains a mixture of intermediate- and high-spin Fe(III), while the σ-bonded phenyl complex is characterized as containing low-spin Fe(III).[68] The remaining compounds in Table XII are all high spin and have $E_{1/2}$ values that shift in the following order: $N_4C(CH_2CH_3) \approx Br^- < N_4C(CH_3) < Cl^- N_3^- < F^- < C_6F_5 < C_6F_4H$.

Correlations between electrochemical data and ^{13}C NMR parameters[78] or Fe(III) binding energies as measured by XPS[79] have been carried out for (TPP)FeX complexes containing the above anionic ligands as well as $OC_6H_5^-$, $O(p\text{-}NO_2C_6H_4)^-$, OAc^-, and NCS^-. The electrochemical data in Table XII are consistent with the order of ligand field strength reported in the literature[78,79] and give further evidence to support an axial anionic-like metal-ligand bond in (P)Fe[$N_4C(R)$]. The spectroscopic and electrochemical data both indicate that the tetrazolato ligand is weaker than either N_3^- or Cl^-, and this conclusion was also reached by an evaluation of the complexes' zero-field splitting.

Concluding Remarks. This study has demonstrated that it is possible to involve the axial azide of an iron porphyrin in a classical organic reaction. The reactions reported in this paper lead to new series of σ-bonded nitrogen iron derivatives which have never before been reported in iron porphyrin chemistry. The electronic configuration of these tetrazolato and triazolato complexes are close to those of the starting $(P)FeN_3$ compounds as well as close to those of other (P)FeX derivatives with anionic axial ligands. The iron atoms of (P)Fe[$N_4C(R)$] and $(P)Fe(N_3C_6H_4)$ are all in a high-spin state and the axial iron-nitrogen bonds all have a slight covalent character. These compounds model the entry of the active site of cytochrome $P\text{-}450_{cam}$ and prove that compounds such as 2-phenylimidazole[37] can inhibit the oxidation of camphor in camphor P-450 with no direct coordination to the heme iron atom.

Acknowledgment. We acknowledge J. Hubsch (Laboratoire de Minéralogie et Cristallographie, Université de Nancy I, France) for the magnetic susceptibility measurements. The support of the CNRS, the National Institutes of Health (K.M.K.; Grant No. GM25172), and Nato (Grant 0168(87)) is also gratefully acknowledged.

Supplementary Material Available: Tables of hydrogen atom fractional coordinates, anisotropic temperature factors, bond distances and angles, and least-squares planes (11 pages); a table of observed and calculated structure factors for $(OEP)Fe[N_4C(CH_3)]$ (6 pages). Ordering information is given on any current masthead page.

(75) Walker, F. A.; La Mar, G. N. *Ann. N.Y. Acad. Sci.* **1973**, *206*, 328.
(76) La Mar, G. N.; Eaton, G. R.; Holm, R. H.; Walker, F. A. *J. Am. Chem. Soc.* **1973**, *95*, 63.
(77) Dolphin, D. H.; Sams, J. R.; Tsin, T. B.; Wong, K. L. *J. Am. Chem. Soc.* **1978**, *100*, 1711.
(78) Goff, H. M.; Shimomura, E. T.; Philippi, M. A. *Inorg. Chem.* **1983**, *22*, 66.
(79) Kadish, K. M.; Bottomley, L. A.; Brace, J. G.; Winograd, N. *J. Am. Chem. Soc.* **1980**, *102*, 4341.

Contribution from the Department of Chemistry, University of Alabama, Tuscaloosa, Alabama 35487-0336

Heteronuclear Multiple-Quantum Coherence NMR Spectroscopy of Paramagnetic Heme and Cytochrome *c*-551

Russell Timkovich

Received April 23, 1990

Heteronuclear multiple-quantum coherence (HMQC), heteronuclear multiple-bond coherence (HMBC), and heteronuclear multiple-quantum relay (HMQR) NMR spectra were obtained for the bis(cyano) complex of iron(III) protoporphyrin IX (dicyanoheme *b*), its free base, horse heart ferricytochrome *c*, and *Pseudomonas aeruginosa* ferricytochrome *c*-551. For the heme it was possible to assign all the protons and carbons. For the hemoproteins, it was possible to assign select protons and carbon atoms near the paramagnetic iron that can act as active-site probes in both the ^1H and ^{13}C frequency regions.

Introduction

Cytochrome *c*-551 is an electron-transport protein that functions in bacteria analogously to cytochrome *c* in mitochondrial electron transport. With 82 amino acid residues as opposed to the ca. 103 for the latter cytochrome, it is a structurally simplified version that performs an equivalent function. One approach toward understanding the structure-mechanism relation in cytochromes is to compare properties for the smaller and larger versions. Examination of the paramagnetically shifted NMR spectra of cytochromes has been an important study in general, because the

0020-1669/91/1330-0037$02.50/0

paramagnetic shifts reveal electronic and geometric structures. The solution structure of the diamagnetic ferrocytochrome *c*-551 from *Pseudomonas aeruginosa* has recently been compared to that of eukaryotic cytochrome *c*.[1] The purpose of the present report is to extend the comparison to the paramagnetic ferricytochromes with emphasis on ^{13}C sites.

Observation of paramagnetically shifted resonances, especially ^{13}C, in proteins has been accomplished, but it is appropriate to say that far less has been done than for diamagnetic macromolecules. The detection and assignment of proton resonances in paramagnetic systems by two-dimensional techniques have been accomplished.[2] One-dimensional ^{13}C spectroscopy and limited assignments have been reported for eukaryotic ferricytochrome *c*.[3] Two-dimensional ^{1}H, ^{13}C correlation spectra with observation at the ^{13}C frequency have been reported with assignments of heme methyls for the met-cyano complex of sperm whale myoglobin,[4] horse heart ferricytochrome *c*,[5] and its cyano complex.[6]

^{1}H heteronuclear scalar correlation spectroscopy with detection at the ^{1}H frequency after polarization transfer (X to ^{1}H) has become a powerful technique for the observation and assignment of insensitive nuclei.[7] For ^{13}C at natural abundance, it has sensitivity advantages over previous techniques such as DEPT, INEPT, or INADEQUATE. To the author's knowledge, it has not been widely applied to paramagnetic molecules. Oh, Mooberry, and Markley have recently observed and assigned select ^{1}H, ^{15}N, and ^{13}C resonances in an isotopically enriched ferrodoxin with a paramagnetic Fe_2–S_2 core.[8] Such applications have potential problems because of the rapid relaxation and large line widths of the proton resonances when compared to those of diamagnetiic samples. Rapid relaxation during the preparation and evolution periods could drastically limit the remaining signal for the detection period. When the line width approaches the magnitude of the ^{1}H heteronuclear coupling constant, the *J*-editing and refocusing steps of pulse sequences become inefficient. The purpose of the present report is to demonstrate that useful information is still obtainable on paramagnetic samples, even small proteins. It has been possible to resolve and assign all the carbons of low-spin bis(cyano)iron(III) protoporphyrin IX. The structure and IUPAC–IUB nomenclature for protoporphyrin IX are given in **1**. In *c*-type cytochromes, the vinyl groups at positions 3 and 8 become thioether bonds to the polypeptide, and positions 3^1 and 8^1 have methine protons with the carbon bonded to the sulfur of cysteine residues, while sites 3^2 and 8^2 are methyl groups. For ferric horse heart cytochrome *c* and cytochrome *c*-551 from *P. aeruginosa*, less detailed information was obtained than for free heme. However, spectra confirm previous assignments of paramagnetically shifted ^{1}H and ^{13}C resonances and reveal new resonances that can serve as probes of the active-site heme environments.

Experimental Section

(Protoporphyrin IX)iron(III) chloride, the free base, and horse heart cytochrome *c* (type VI) were purchased from the Sigma Chemical Co., St. Louis, MO. Cytochrome *c*-551 was purified from *P. aeruginosa*

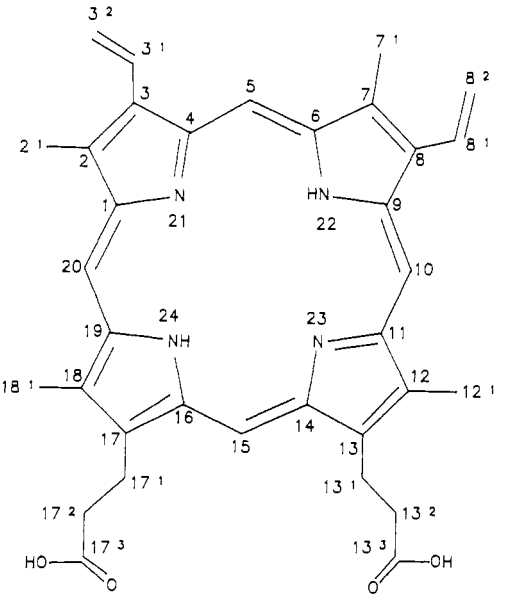

1

(ATCC 19429) as described previously.[9] The heme (final concentration 15 mM) was dissolved in 0.75 mL of pyridine-$4d_5$, to which was added 0.25 mL of deuterium oxide saturated with potassium cyanide and 0.15 mL of pure deuterium oxide. The free base (17 mM) was dissolved in pyridine-d_5. Values of pH were measured with a glass electrode calibrated against normal protic standards and were not corrected for isotope effects. The proteins (final concentration 10 mM) were lyophilized from 50 mM ammonium bicarbonate solutions, redissolved in 99.8% deuterium oxide buffered with 50 mM potassium phosphate to pH 7.0, lyophilized directly from 5-mm NMR sample tubes, and then redissolved in 99.996% deuterium oxide (Cambridge Isotope Laboratories). This procedure greatly suppresses the residual water resonances. In addition, the *c*-551 sample contained 75 mM potassium ferricyanide. This was necessary in order to ensure complete oxidation of the cytochrome. Traces of reduced cytochrome are present after the final purification and cause severe line broadening due to chemical exchange between oxidized and reduced states.[10] Control experiments indicated that, at these concentrations, the ferricyanide did not act as a significant relaxation of external paramagnetic shift reagent on the protein resonances.

Spectra were recorded on Bruker AM 360 and AM500 spectrometers, and hardware configurations have been described.[11] Long-range ^{1}H–^{13}C scalar correlation spectra (heteronuclear multiple-bond correlations, or HMBC) were recorded with the pulse sequence of Summers et al.[7] Direct ^{1}H–^{13}C scalar concentration spectra (heteronuclear multiple-quantum correlations, or HMQC) were recorded with slight modifications of the pulse sequence of Bax, Griffey, and Hawkins,[12] in which the phase of the first 90° ^{13}C pulse was incremented by 90° with t_1 increments to achieve phase-sensitive detection in F1 by the TPPI method,[13] and ^{13}C decoupling during acquisition was accomplished by a GARP-1 sequence.[14] Relayed ^{1}H–^{13}C scalar correlation spectra (HMQR) were recorded by a modification of sequence 1a of Lerner and Bax.[15] The actual sequence was

$$D1\text{-}90_a(^{13}C)90_b(^{1}H)\text{-}D2\text{-}90_c(^{13}C)\text{-}t_1/2\text{-}180_d(^{1}H)\text{-}t_1/2\text{-}90_e(^{13}C)\text{-}D2\text{-}90_f(^{1}H)\text{-}acq_g(^{1}H)\text{-}t_2$$

where D1 was a relaxation delay and D2 was approximately $1/^{1}J(^{1}H$–$^{13}C)$, or typically 3.6 ms. The letter subscripts represent the pulse phases, which were cycled as follows: a = *x*, *x*, *x*, *x*, −*x*, −*x*, −*x*, −*x*; b = *x*; c = x, −*x*; d = *x*; e = *x*, *x*, −*x*, −*x*; f = *y*; g = +, −, −, +. In addition, phase c was incremented by 90° with t_1 increments to achieve phase-sensitive spectra by the TPPI method. No ^{13}C decoupling was applied during acquisition, and one bond coupling was not suppressed. The resultant

(1) (a) Chau, M. H.; Cai, M. L.; Timkovich, R. *Biochemistry* **1990**, *29*, 5076. (b) Timkovich, R. *Biochemistry* **1990**, *29*, 7773.
(2) (a) Santos, H.; Turner, D. L.; Xavier, A. V. *J. Magn. Reson.* **1984**, *59*, 177. (b) Peters, W.; Fuchs, M.; Sicius, H.; Kuchen, W. *Angew. Chem., Int. Ed. Engl.* **1985**, *24*, 231. (c) Jenkins, B. G.; Lauffer, R. B. *J. Magn. Reson.* **1988**, *80*, 328. (d) Jenkins, B. G.; Lauffer, R. B. *Inorg. Chem.* **1988**, *27*, 4730. (e) Emerson, S. D.; La Mar, G. N. *Biochemistry* **1990**, *29*, 1545.
(3) (a) Oldfield, E.; Norton, R. S.; Allerhand, A. *J. Biol. Chem.* **1975**, *250*, 6381. (b) Burch, A. M.; Rigby, S. E.; Funk, W.; MacGillivray, R. T. A.; Mauk, A. G.; Mauk, M.; Moore, G. R. *Biochem. Soc. Trans.* **1988**, *16*, 844.
(4) Yamamoto, Y. *FEBS Lett.* **1987**, *222*, 115.
(5) Santos, H.; Turner, D. L. *FEBS Lett.* **1986**, *194*, 73.
(6) Yamamoto, Y.; Nanai, N.; Inoue, Y.; Chujo, R. *Biochem. Biophys. Res. Commun.* **1988**, *151*, 262.
(7) Summers, M. F.; Marzilli, L. G.; Bax, A. *J. Am. Chem. Soc.* **1986**, *108*, 4285.
(8) (a) Oh, B. H.; Markley, J. L. *Biochemistry* **1990**, *29*, 3993. (b) Oh, B. H.; Mooberry, E. S.; Markley, J. L. *Biochemistry* **1990**, *29*, 4004. (c) Oh, B. H.; Markley, J. L. *Biochemistry* **1990**, *29*, 4012.
(9) Timkovich, R.; Dhesi, R.; Martinkus, K. A.; Robinson, M. K.; Rea, T. *Arch. Biochem. Biophys.* **1982**, *215*, 45.
(10) Timkovich, R.; Cai, M. L.; Dixon, D. W. *Biochem. Biophys. Res. Commun.* **1988**, *150*, 1044.
(11) Timkovich, R.; Bondoc, L. L. *Magn. Reson. Chem.* **1989**, *27*, 1048.
(12) Bax, A.; Griffey, R. H.; Hawkins, B. L. *J. Magn. Reson.* **1983**, *55*, 301.
(13) Marion, D.; Wuthrich, K. *Biochem. Biophys. Res. Commun.* **1983**, *113*, 967.
(14) Shaka, A. J.; Barker, P. B.; Freeman, *J. Magn. Reson.* **1985**, *64*, 547.
(15) Lerner, L.; Bax, A. *J. Magn. Reson.* **1986**, *69*, 375.

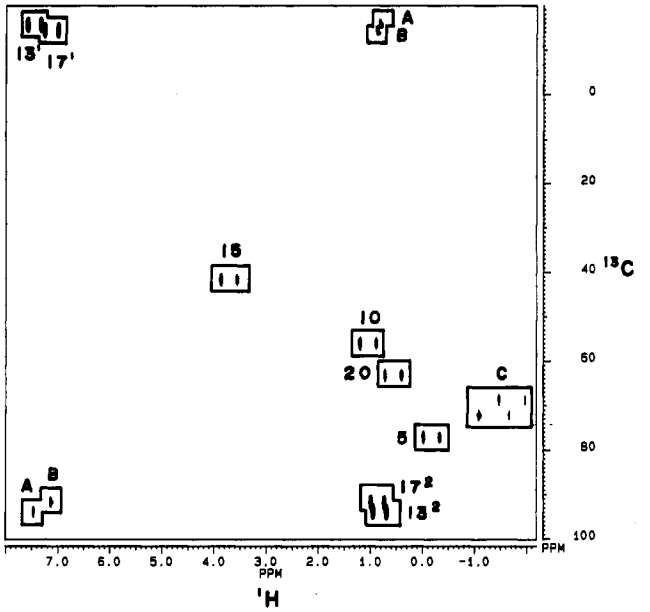

Figure 1. Portion of the HMQR spectrum of bis(cyano)iron(III) protoporphyrin IX. Peaks with numeric labels correspond to direct $^1H-^{13}C$ correlation peaks for the heme resonances given with IUB–IUPAC nomenclature. They appear as absorptive doublets with $^1J(^1H,^{13}C)$ parallel to the proton axis. The cross peak labeled A is a relay peak between the site 13^1 and 13^2 spin systems. Relay peaks have a dispersive shape, but only the positive contours have been drawn. B is a relay beak between sites $1'^1$ and 17^2. C is a cluster of relay peaks involving the vinyl chains at sites 3 and 8, but the direct peaks lie outside the plotted region. Peaks labeled 5, 10, 15, and 20 are direct peaks for the meso sites.

spectra show cross peaks due to $^1J(^1H-^{13}C)$ as absorptive in-phase doublets along F2 and cross peaks due to relayed transfer as dispersive antiphase multiplets. Pulse sequences such as 1b of Lerner and Bax[8] that employ a spinlock to achieve relay transfer by the homonuclear Hartmann–Hahn mechanism did not perform as well in the present study because of relaxation during the spinlock period. The heteronuclear RELAY experiments proposed by Bruhwiler and Wagner[16] seemed to suffer a similar problem in that signals relaxed during the homospoil recovery delay.

All spectra were recorded at 32 °C with ^1H and ^{13}C transmitters placed in the center of the range of resonances. Eight dummy scans were recorded but not saved to establish a steady state of longitudinal magnetization. Typically, 2048 or 4096 data points were collected in the t_2 dimension and 200–256 points in t_1. HMBC spectra were apodized by a sine bell function in F2 and no apodization in F1. Other spectra were apodized by squared 60° shifted sine functions in both F2 and F1. Chemical shifts for both ^1H and ^{13}C resonances were referenced versus sodium 3-(trimethylsilyl-d_4)-propionate (TSP). In certain cases, internal TSP could not be added to the sample because it would obscure relevant resonances near zero ppm. For these, an equivalent sample was prepared and routine one-dimensional spectra were recorded to obtain shifts for sample resonances that were then applied to reference two-dimensional spectra. Initial spectra were recorded with large spectral widths in the ^{13}C dimension. The pulse sequences, especially HMBC and HMQR, do not distinguish folded-in cross peaks, and in light of the unusual ^{13}C shift values and large range, an initial determination of the proper spectral window was important.

Results and Discussion

Suppression of signals due to $^1H-^{12}C$ to avoid dynamic range limitation is an important aspect of polarization-transfer techniques. Methods such as BIRD[17] are not appropriate for paramagnetic samples because of the fast relaxation. However, the fast relaxation may be exploited to suppress substantial contributions to the free induction decay without sacrificing paramagnetically shifted signals. It was observed that short acquisition times (5–9 ms) and short delays after acquisiition (5–150 ms) led to saturation of proton signals not affected by the paramagnetic center. For the heme, these were solvent resonances. For the protein, most protons are distant from the ferric iron and their suppression becomes more critical. For paramagnetically shifted resonances, rapid pulsing does not suppress the central $^1H-^{12}C$ peak relative to the $^1H-^{13}C$ satellites, but it does remove other signals to the point where phase cycling can accomplish this. The relaxation delay was adjusted to minimize free induction decay intensity while maintaining an acceptable signal-to-noise ratio for paramagnetically shifted resonances observed in normal one-dimensional proton spectra.

Figure 1 shows a section of the HMQR spectrum of bis(cyano)iron(III) protoporphyrin IX, and Figure 2 shows a section of the HMBC spectrum. Assignments derived from these are given in Table I. Numerical values for shifts were taken from high-resolution one-dimensional spectra. The table also gives assignments for the free base to indicate the magnitude of the paramagnetic contributions for the heme. Only a qualitative comparison is intended at the present time. Although there is high solubility, pyridine is not an ideal NMR solvent for the free base, because of overlap of resonances. The esterified porphyrin in halogenated solvents shows greater shift dispersion.

Table I. NMR Assignments for Bis(cyano)iron(III) Protoporphyrin IX and the Free-Base Porphyrin[a]

	heme		free base	
assgn	^1H	^{13}C	^1H	^{13}C
5	−0.19	77.86	10.38 or 10.36[b]	99.20 or 98.70
10	1.03	57.57	10.38 or 10.36	99.20 or 98.70
15	3.70	42.94	10.71	98.78
20	0.55	64.16	10.22	98.65
2^1	11.45	−22.76	3.63 or 3.61[c]	13.48
7^1	12.99	−25.96	3.60	12.38
12^1	16.71	−35.04	3.60	12.38
18^1	17.19	−35.58	3.63 or 3.61	13.48
3^1	12.08	69.65	8.41[d]	131.52
3^{2a}	−1.49	165.57	6.40	121.75
3^{2b}	−1.99		6.16	
8^1	11.22	73.05	8.41	131.52
8^{2a}	−1.11	162.40	6.40	121.75
8^{2b}	−1.68		6.16	
13^1	7.45	−14.91	4.27[e]	23.32
13^2	0.80	93.89	3.59	38.71
13^3		187.24		176.36
17^1	7.12	−13.65	4.27	38.71
17^2	0.83	91.74	3.59	23.31
17^3		187.48		176.36
2		108.70		138[f]
3		134.65		138
7		124.88		138
8		118.94		138
12		138.12		138
13		127.29		141.20
17		122.34		141.20
18		142.84		138
1		50.98		146[g]
4		34.49		146
6		40.44		146
9		50.29		146
11		39.46		146
14		57.01		146
16		58.70		146
19		33.07		146

[a] Chemical shifts in ppm from TSP at 32 °C. [b] Because of overlap, protons 5 and 10 could not be uniquely assigned. However, the 99.20 ppm carbon is attached to the 10.38 ppm proton. [c] Because of overlap the specific methyls could not be uniquely assigned. Only two ^{13}C peaks appear at the methyl resonance positions 13.48 and 12.38 ppm, even in the highest resolution one-dimensional spectra that could be atttained. The two highest frequency methyl proton resonances are attached to the 13.48 ppm carbons. [d] The vinyl 3 and 8 substituents are degenerate in both ^1H and ^{13}C spectra. [e] Propionates 13 and 17 are degenerate in both ^1H and ^{13}C spectra. [f] The β-carbons are highly overlapped and appear as a broad envelope centered at about 138 ppm. Two are resolved at 141.2 ppm and can be assigned to sites 13 and 17 on the basis of a cross peak in the HMBC spectrum from protons 13^1 and 17^1. [g] The α-carbons are highly overlapped and appear as a broad cluster centered at about 146 ppm.

(16) Bruhwiler, D.; Wagner, G. *J. Magn. Reson.* **1986**, *69*, 546.
(17) Bax, A.; Subramanian, S. *J. Magn. Reson.* **1986**, *67*, 565.

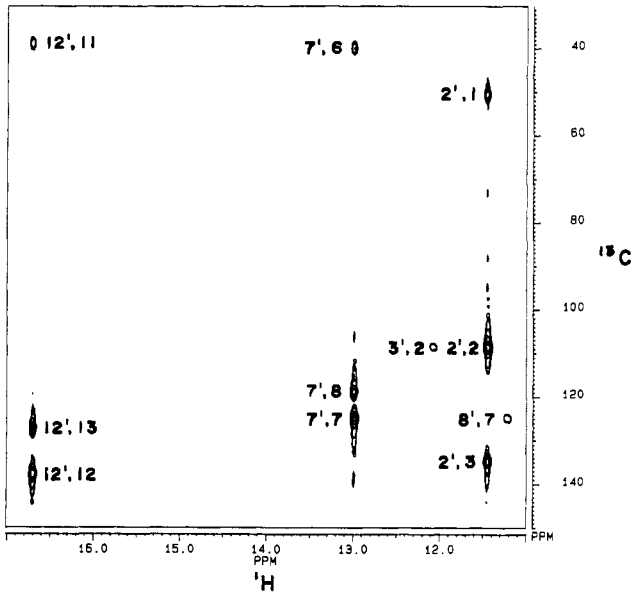

Figure 2. Portion of the HMBC spectrum of bis(cyano)iron(III) protoporphyrin IX. The peaks are labeled with two coordintes. The first is the IUB-IUPAC nomenclature for the carbon with attached proton, and the second is for the nonprotonated carbon whose chemical shift is then given along the carbon axis. For example, the peak labeled 12^1,13 demonstratcs the chemical shift of protons 12^1 along the horizontal axis and the coherence transferred to the carbon 13, whose shift is given along the vertical axis. The peaks have magnitude mode line shapes. In order to show the weaker peaks, the minimum contour level was decreased and the strong peaks then show tailing and t_1 ridges.

The interpretation of HMQR spectra was straightforward. Cross peaks due to one-bond coupling $^1J(^1H_a-^{13}C_x)$ were readily assigned at coordinates (^1H_a, $^{13}C_x$) because of their absorptive phase and the splitting along F2. In the following discussion the superscript on J is the number of bonds between the coupled nuclei. Examples of ^1J in Figure 1 include peaks for the propionate substituents labeled 13^1 and 17^1. Cross peaks due to relayed coherence transfer appeared for fragments $H_a-C_x\cdots C_y-H_b$ at shift coordinates (^1H_b, $^{13}C_x$) and (^1H_a, $^{13}C_y$) if $^3J(^1H_a-^1H_b)$ was not zero. Examples in Figure 1 include the cross peaks labeled A and B. HMBC spectra gave cross peaks due to long-range coupling, $^2J(^1H_a-^{13}C_y)$ or $^3J(^1H_a-^{13}C_z)$, for fragments $H_a-C_x\cdots C_y\cdots C_z$, regardless of whether C_y or C_z had attached protons, as magnitude mode singlets, at coordinates (^1H_a, $^{13}C_y$) and (^1H_a, $^{13}C_z$). Examples in Figure 2 include the peaks correlating the methyl group at position 12^1 with the nonprotonated carbons at positions 11, 12, and 13. As pointed out by Summers et al.,[7] cross peaks at (^1H_a, $^{13}C_x$) due to $^1J(^1H_a-^{13}C_x)$ are only partially suppressed by the HMBC sequence, depending upon the match between the pulse sequence delay in the J filter and the actual value of ^1J. The ^1J cross peaks were readily recognized as such because they retain the ^1J splitting along F2. The greatest difficulty in intepreting HMBC spectra for the porphyrins was the fact that cross peaks due to ^3J could be much stronger than peaks due to ^2J and some ^2J cross peaks were not observed. This occurred because in olefinic systems ^2J can be less than 1 Hz, while ^3J can be 5–6 Hz. Such a situation has been observed in vitamin B_{12}.[7] The following trends applied to both the paramagnetic heme and the diamagnetic porphyrin. A meso proton such as that at position 5 showed cross peaks to β-carbons 3 and 7 (^3J), but not to α-carbons 4 and 6 (^2J) on the adjacent pyrroles. Methyl protons such as those at position 2^1 showed the strongest cross peak to β-carbon 2 (^2J), but the cross peak to the next β-carbon, carbon 3 (^3J), was also very strong. The cross peak to α-carbon 1 (^3J) was very weak. Vinyl protons such as those at position 3^2 showed a strong cross peak to carbon 3^2 but a weak peak to carbon 3. Propionate protons such as that at position 13^1 showed strong peaks to both carbons 13^1 and 13, a moderate peak to carbon 12, but a very weak peak to carbon 14. Protons 13^2 showed strong peaks to both carbons 13^3 and 13^1 and a weak peak to carbon 13.

^{13}C resonances for bis(cyano)iron(III) protoporphyrin IX have been assigned for the heme methyls in detail and for others by type,[18] and ^1H resonances have been extensively assigned by selective deuteration and nuclear Overhauser enhancements to specific protons[19] although ambiguities regarding positions 17^2 versus 13^2 and 8^2 versus 3^2 were not settled. The specific carbon assignments required the heteronuclear correlation spectra, but an interesting question is whether the ^1H assignments could be made independent of the previous results. The following analysis indicates an affirmative answer.

Methyl, methylene, methine, and vinyl protons were assignable by type from the observed relay cross peaks or lack thereof in HMQR spectra. Methyl and methine ^1H resonances were readily differentiated on the basis of ^1H intensity. HMQR cross peaks did not distinguish protons 13^1 from protons 13^2 or protons 17^1 from protons 17^2, but the large paramagnetic shift for the inner methylene and the attached carbon indicated which was closest to the iron. HMQR cross peaks distinguished protons 8^1 from $8^{2a,b}$, because the latter presented two ^1H resonances at a single ^{13}C shift value. Also the intensity of the cross peaks (trans coupling greater than cis) marked proton 8^{2a}. In HMBC spectra, meso proton 20 was unique in showing ^3J coupling to two carbons, carbons 2 and 18, that also showed ^2J coupling to two methyls, sites 2^1 and 18^1. The methyls could be differentiated because methyl 2^1 showed ^3J coupling to site 3 and site 3 is ^2J-coupled to site 3^1. Site 18^1 was coupled to site 17, which in turn was coupled to site 17^1. The pattern assigned the site 3 vinyl and site 17 protons and carbons. The site 15 meso proton was next assigned by its ^3J coupling to carbons 17 and 13. The site 5 meso proton was assigned by its ^3J coupling to carbons 3 and 7, and then the assignment for site 7^1 followed from the site 7^1, 7 cross peak. Assignments for sites 10, 8, and 13 followed by similar reasoning. This order of analysis was not unique, and identical conclusions may be obtained by beginning at any porphyrin substituent and following the coupling pattern around the ring. For bis(cyano)iron(III) protoporhyrin IX, the patterns in HMQR and HMBC were sufficiently distinctive to assign both carbon and proton resonances largely independent of chemical shift analogies and independent of $^1H-^1H$ nuclear Overhauser enhancements. This may not always be the case, but it does illustrate the potential of the heteronuclear correlation approach for paramagnetic systems.

Application of HMQC and HMQR to the paramagnetic proteins horse heart cyt *c* and *P. aeruginosa* cyt *c*-551 gave lower signal-to-noise ratios than for the heme, because of the decrease in relaxation time. However, as illustrated in Figures 3 and 4, rich spectral detail was still obtained. The quality of HMBC spectra for the proteins was very poor, and no useful information was obtained. ^1H assignments have been previously made for paramagnetically shifted resonances in both horse heart cyt *c* and cyt *c*-551.[20,21] These allow the attached carbon to the assigned as presented in Table II. ^{13}C methyl assignments agree with a previous report for horse heart cytochrome *c*.[5] The information

(18) (a) Wuthrich, K.; Baumann, R. *Helv. Chim. Acta* **1974**, *57*, 336. (b) La Mar, G. N.; Viscio, D. B.; Smith, K. M.; Caughey, W. S.; Smith, M. L. *J. Am. Chem. Soc.* **1978**, *100*, 8085.

(19) (a) Barbush, M.; Dixon, D. W. *Biochem. Biophys. Res. Commun.* **1985**, *129*, 70 and references cited therein. (b) Yu, C.; Unger, S. W.; La Mar, G. N. *J. Magn. Reson.* **1986**, 346.

(20) (a) Redfield, A. G.; Gupta, A. *Cold Spring Harbor Symp. Quant. Biol.* **1971**, *36*, 405. (b) Keller, R. M.; Wuthrich, K. *Biochim. Biophys. Acta* **1978**, *533*, 195. (c) Moore, G. R.; Williams, G. *Biochim. Biophys. Acta* **1984**, *788*, 147. (d) Williams, G.; Moore, G. R.; Porteous, R.; Robinson, M. N.; Soffe, N.; Williams, R. J. P. *J. Mol. Biol.* **1985**, *183*, 409. (e) Feng, Y.; Roder, H.; Englander, S. W.; Wand, A. J.; DiStefano, D. L. *Biochemistry* **1989**, *28*, 195. (f) Satterlee, J. D.; Moench, S. *Biophys. J.* **1987**, *52*, 101. (g) Santos, H.; Turner, D. L. *FEBS Lett.* **1987**, *226*, 179. (h) Feng, Y.; Roder, H.; Englander, S. W. *Biophys. J.* **1990**, *57*, 15.

(21) (a) Keller, R. M.; Wuthrich, K.; Pecht, I. *FEBS Lett.* **1976**, *70*, 180. (b) Moore, G. R.; Pitt, R. C.; Williams, R. J. P. *Eur. J. Biochem.* **1977**, *77*, 53. (c) Keller, R. M.; Wuthrich, K. *Biochem. Biophys. Res. Commun.* **1978**, *83*, 1132. (d) Moore, G.; Pettigrew, G. W.; Pitt, R. C.; Williams, R. J. P. *Biochim. Biophys. Acta* **1980**, *590*, 261. (e) Leitch, F. A.; Moore, G. R.; Pettigrew, G. W. *Biochemistry* **1984**, *23*, 1831.

Table II. Resonance Assignments from Heteronuclear Correlation Spectra for Horse Heart cyt *c* and *P. aeruginosa* cyt *c*-551[a]

cyt *c*-551			horse heart cyt *c*		
assgn	^1H	^{13}C	assign	^1H	^{13}C
2^1	24.80[21c]	−46.9	2^1	7.37[20b]	−16.6[5]
7^1	13.47[21c]	−21.8	7^1	31.53[20b]	−51.4[5]
12^1	31.25[21c]	−54.3	12^1	10.19[20b]	−22.4[5]
18^1	17.17[21c]	−35.9	18^1	34.22[20b]	−65.3[5]
$17^{1a,b}$	12.98,[21e] 11.03[21e]	−23.3	$17^{1a,b}$	18.35,[20c,f] 11.31[20c,f]	−30.5
3^1	3.88	−1.8		1.28[20h]	
3^2	2.63[21c]	62.8	3^2	−2.25[20b]	40.2[5]
8^1	−1.00	−22.2	8^1	2.49	−33.5
8^2	−0.13[21c]	69.6	8^2	3.05[20b]	83.1[5]
His 16 C_α	8.14	74.7	His 18 C_α	8.56[20c,f]	74.9
His 16 $C_{\beta 1,2}$	8.24, 6.50	26.1	His 18 $C_{\beta 1,2}$	13.99,[20c,f] 8.24[20c,f]	26.3
Met 61 CH_3	−16.38[21a,b]	68.1	Met 80 CH_3	−23.49[20a,b]	
Met 61 $C_{\beta 1,2}$	5.26, 0.83	0.2	Met 80 $C_{\beta 1,2}$	11.97,[20e,g] 6.70	6.6
Gly 24 $C_{\alpha 1,2}$	−0.27, −3.02	28.4	Gly 29 $C_{\alpha 1,2}$	−4.07,[20e,g] −0.51[20e,g]	36.7
Pro 25 C_δ	−2.57	61.5	Pro 30 $C_{\delta 1,2}$	−6.05,[20e,g] −2.11[20e,g]	46.1
			Leu 68 CH_3	−2.60[20d]	18.8

[a] Chemical shift values are in ppm from TSP at 32 °C. Superscript literature citations refer to previous publications where assignments were made or proposed. In some cases indpendent assignment evidence has been acquired by different groups and published at different times. Cross citations may be found in the cited works.

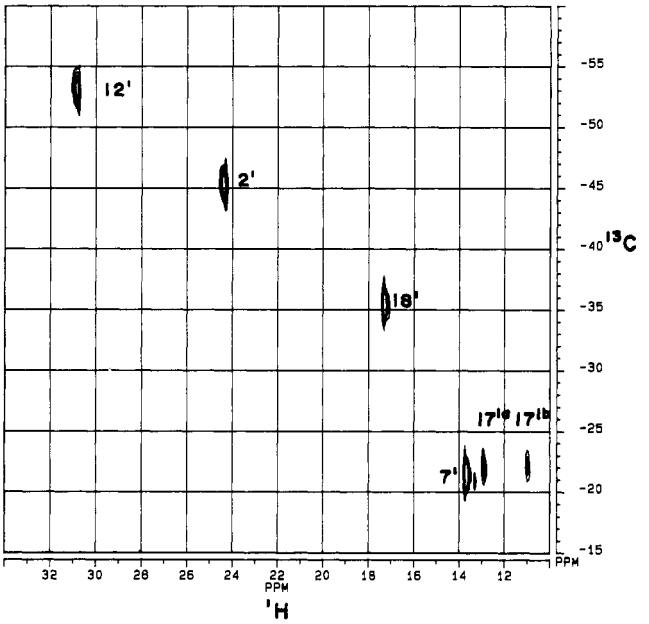

Figure 3. Portion of the HMQC spectrum of ferricytochrome *c*-551 from *P. aeruginosa* at neutral pH and 32 °C. Heme methyl resonances and the propionate $17^{1a,b}$ resonances are shown to demonstrate the distinctive appearance of geminal protons.

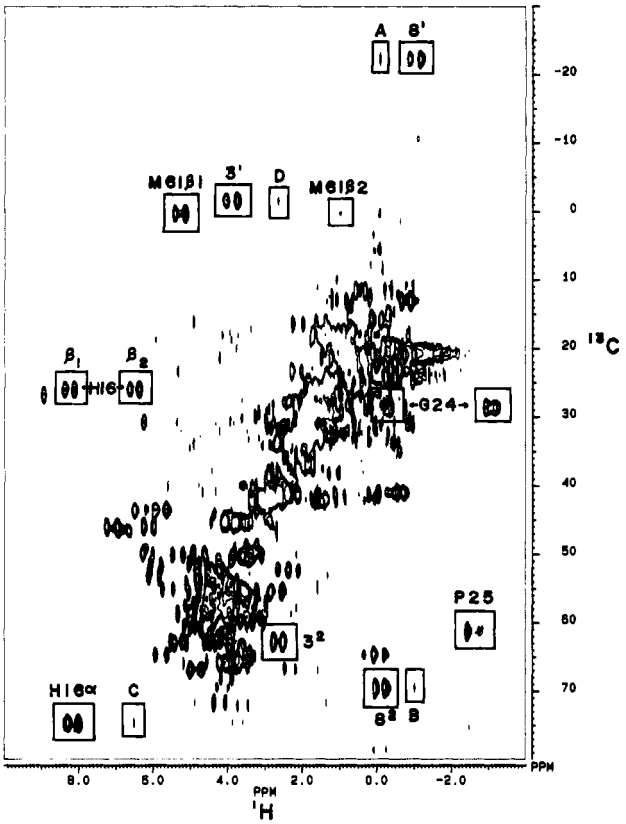

Figure 4. Portion of the HMQR spectrum of *P. aeruginosa* ferricytochrome *c*-551. Several distinctive direct correlation peaks have been marked for His 16 C_α, $C_{\beta 1}$, and $C_{\beta 2}$, Met 61 $C_{\beta 1}$ and $C_{\beta 2}$, Gly 24 $C_{\alpha 1}$ and $C_{\alpha 2}$, and thioethers 3^1, 8^1, 3^2, and 8^2. Peaks A and B are relay peaks for thioether 8, peak D is for thioether 3, and peak C is a relay peak between the His 61 C_α and $C_{\beta 2}$. The peak labeled Met 61 $C_{\beta 2}$ is a direct coherence transfer peak but appears weak in this plot due to a negative t_1 ridge that runs through it, arising from intense methyl signals around 1 ppm.

in HMQC and HMQR spectra provided corroboration and additional ^1H and ^{13}C assignments. For example, as shown in Figure 3, geminal protons such as those at $17^{1a,b}$ are distinctive in HMQC spectra because they correlate with the same ^{13}C shift. New assignments of both ^1H and ^{13}C resonances were also made. The assignment of horse heart cyt *c* Met 80 $C_{\beta 2}$ at 6.70 ppm was based on a correlation with the carbon at 6.6 ppm in a noncrowded spectral window, and this carbon is attached to the unique β-proton at 11.97 ppm for which there is consensus assignment to Met 80.[20] This does not agree with a previous assignment of the proton to 3.0 ppm.[20g] The assignments of His 16, Gly 24, Pro 25, and Met 61 $C_{\beta 1,2}$ in cyt *c*-551 were based on analogy to horse heart cyt *c* resonances. The two proteins share a common structure around the heme on the basis of X-ray crystal structures.[22] Relay peaks in HMQR spectra provided assignment evidence as illustrated in Figure 4. A relay peak (labeled C) from the His 16 C_α to the His 16 $C_{\beta 2}$ indicated the resonances were correlated. This type of relay information was important for assigning site 8^1, 8^2, 3^1, and 3^2 resonances in both horse heart cyt *c* and *c*-551. Figure 4 shows the relay peaks (A, B) between the site 8^1 and 8^2 spin systems. No relay peak above the noise level was observed from site 3^2 in horse heart cyt *c*, so an assignment to site 3^1 was not made. An unassigned peak at −0.58 (^1H) and 0.76 (^{13}C) ppm could be a candidate.

The heteronuclear correlation spectra for the proteins failed to reveal carbon correlatioins for some of the broadest proton peaks. For example, a correlation peak was observed for the Met

(22) Matsuura, Y.; Takano, T.; Dickerson, R. E. *J. Mol. Biol.* **1982**, *156*, 389.

61 methyl in cyt c-551, but not for the Met 80 methyl in horse heart cyt c. For both cytochromes, additional broad proton peaks in the low-frequency region did not give rise to correlation peaks above the spectral noise level. There are only a few of these however, and they are believed to be protons on the ligand methionine and histidine side chains that are very close to the iron. From the detail in Figure 4, it is clear that much remains to be done. One-dimensional ^1H spectra of paramagnetically shifted resonances in hemoproteins and iron-sulfur proteins have long been used to probe the active-site region. The dispersion of carbon resonances adds a new dimension and adds new probe resonances that may be followed during ligand changes, spin-state changes, and conformational changes in the active-site region.

A detailed interpretation of the contact and pseudocontact shifts for the heme or proteins is beyond the present scope. Several excellent reviews of theory have been given.[23] It has long been known, and is highlighted by comparing Tables I and II, that free heme and hemoproteins are very different because of the influence of the protein. The addition of carbon chemical shift data to the analysis may afford a better description of the electronic environment at the protein active site.

Acknowledgment. Financial support was provided in part by Grant GM 36264 from the National Institutes of Health.

Registry No. Cytochrome c-551, 9048-77-5; cytochrome c, 9007-43-6; dicyanoheme b, 130523-00-1; protoporphyrin IX, 553-12-8.

(23) (a) La Mar, G. N.; Walker, F. A. In *The Porphyrins*; Dolphin, D., Ed.; Academic: New York, 1979; Vol. IV, p 61. (b) Goff, H. M. In *Iron Porphyrins*; Leber, A. P. B., Gray, H. B., Eds.; Addison-Wesley: New York, 1983; p 239. (c) La Mar, G. N., Horrocks, W. D., Holm, R. H., Eds. *NMR of Paramagnetic Molecules*; Academic: New York, 1973.

Contribution from the Department of Chemistry and Biochemistry, University of California, Los Angeles, California 90024-1569, and Anorganisch Chemisch Laboratorium, J. H. van't Hoff Instituut, University of Amsterdam, Nieuwe Achtergracht 166, 1018 WV Amsterdam, The Netherlands

Photophysical Properties of a Series of $(CO)_5Re-Re(CO)_3(\alpha,\alpha'$-diimine) Compounds

Londa J. Larson,[†] Ad Oskam,*[,‡] and Jeffrey I. Zink*[,†]

Received March 14, 1990

The electronic absorption and emission spectra of a series of $(CO)_5Re-Re(CO)_3(\alpha,\alpha'$-diimine) compounds as powders and 2-methyltetrahydrofuran glasses at temperatures ranging from 4.2 K to room temperature are reported. The lowest energy absorption band from these compounds is assigned to a composite band of the lowest metal to $\pi_1^*(\alpha,\alpha'$-diimine) charge-transfer (MLCT) transitions. Emission from these compounds is assigned to a MLCT excited state. $Re_2(CO)_8(2,2'$-bpy), $Re_2(CO)_8(4,4'$-Me_2bpy), $Re_2(CO)_8$(1,10-phen), and $Re_2(CO)_8$(isopr-Pyca) exhibit both fluorescence and phosphorescence from this excited state, whereas only phosphorescence is observed from $Re_2(CO)_8$(isopr-DAB) and $Re_2(CO)_8$(ptol-DAB).

Introduction

Excited-state properties of metal-metal-bonded compounds are the subject of continuing interest. The most extensive studies of metal-metal-bonded compounds have involved investigations of their photochemical reactivities.[1,2] Luminescence[3,4] and resonance Raman spectroscopy[5-7] have also been used to characterize the excited states.

The series of bimetallic compounds of the type $M(CO)_5M'(CO)_3(\alpha,\alpha'$-diimine) (M,M' = Mn, Re), where two carbonyls of the parent decacarbonyl compound have been replaced by a bidentate diimine ligand, are of particular relevance to the work in this paper. A variety of these compounds have been synthesized and studied.[5,8] This series of compounds exhibits intense low-energy metal to α,α'-diimine ligand charge-transfer (MLCT) bands in the visible region of the electromagnetic spectrum.[3,5,8] Although, in general, MLCT excited states are unreactive, irradiation into the MLCT band of these compounds causes splitting of the metal-metal bond as well as CO loss.[3,9-12] Under certain conditions metal-nitrogen bond breaking has also been observed.[9] Relatively little is known about the luminescence properties of metal-metal-bonded species with low-lying MLCT excited states. The emission spectrum of $Re_2(CO)_8$(1,10-phen) was measured by Morse and Wrighton in EPA at 77 K.[3] Exciting into the MLCT band yielded emission with a maximum at about 14 500 cm^{-1} and a lifetime of 95 μs. The emission was independent of excitation wavelength. The long lifetime is consistent with emission from a ^{3}MLCT excited state.

In this paper, the luminescence and absorption spectra of a series of $Re_2(CO)_8L$ (L = α,α'-diimine) compounds from powders and from 2-methyltetrahydrofuran (2-MeTHF) glasses at temperatures ranging from 4.2 K to room temperature are reported. The compound structure and the α,α'-diimine ligands are shown in Chart I. For clarity, only the nitrogen atoms of the α,α'-diimine ligand are shown in the structure of the metal compound. The ligands are (a) 2,2'-bipyridine (2,2'-bpy), (b) 4,4'-dimethyl-2,2'-bipyridine (4,4'-Me_2bpy), (c) 1,10-phenanthroline (1,10-phen), (d) R-pyridine-2-carbaldehyde imine (R = isopropyl, isopr-Pyca), and (e) R-1,4-diaza-1,3-butadiene (R = isopropyl, isopr-DAB; R = p-tolyl, ptol-DAB). Multiple emission bands are observed. Single-crystal absorption spectra of $Re_2(CO)_8(2,2'$-bpy) are examined in detail. The emission and lowest energy absorption bands are assigned and the emission lifetimes, temperature and excitation wavelength dependences, and medium effects are discussed.

Experimental Section

Synthesis. The ligands[13] and binuclear metal compounds[3,8] were synthesized according to published methods. A mixture of 2 mmol of $Re(CO)_5^-$ and 1.8 mmol of $Re(CO)_3(\alpha,\alpha'$-diimine)Br in 40 mL of THF was stirred for 2 days. The solvent was evaporated under vacuum and the product purified by column chromatography. Chromatographic separations were carried out with silica gel as the stationary phase. The silica gel was dried, deoxygenated, and activated before use by heating

[†] University of California.
[‡] University of Amsterdam.

(1) Meyer, T. J.; Caspar, J. V. *Chem. Rev.* **1985**, *85*, 187.
(2) Stufkens, D. J. *Coord. Chem. Rev.* **1990**, *104*, 39.
(3) Morse, D. L.; Wrighton, M. S. *J. Am. Chem. Soc.* **1976**, *98*, 3931.
(4) Steigman, A. E.; Miskowski, V. M. *J. Am. Chem. Soc.* **1988**, *110*, 4053.
(5) Kokkes, M. W.; Snoek, T. L.; Stufkens, D. J.; Oskam, A.; Chritophersen, M.; Casper, H. S. *J. Mol. Struct.* **1985**, *131*, 11.
(6) Shin, K.-S.; Clark, R. J. H.; Zink, J. I. *J. Am. Chem. Soc.* **1989**, *111*, 4244.
(7) Yoo, C.-S.; Zink, J. I. *Inorg. Chem.* **1983**, *22*, 2476.
(8) Staal, L. H.; van Koten, G.; Vrieze, K. *J. Organomet. Chem.* **1979**, *175*, 73.
(9) Kokkes, M. W.; Stufkens, D. J.; Oskam, A. *Inorg. Chem.* **1985**, *24*, 2934.
(10) Kokkes, M. W.; Stufkens, D. J.; Oskam, A. *Inorg. Chem.* **1985**, *24*, 4411.
(11) Kokkes, M. W.; De Lange, Wim G. J.; Stufkens, D. J.; Oskam, A. *J. Organomet. Chem.* **1985**, *294*, 59.
(12) Kokkes, M. W.; Brouwers, A. M. F.; Stufkens, D. J.; Oskam A. *J. Mol. Struct.* **1984**, *115*, 19.
(13) Bock, H.; tom Dieck, H. *Chem. Ber.* **1967**, *100*, 228.

0020-1669/91/1330-0042$02.50/0